Stability of dislocation defect with two pentagon-heptagon pairs in graphene

Byoung Wook Jeong,[1] Jisoon Ihm,[1] and Gun-Do Lee[2]
[1]*Department of Physics and Astronomy, Seoul National University, Seoul, 151-742, Republic of Korea*
[2]*Department of Materials Science and Engineering and Inter-University Semiconductor Research Center (ISRC), Seoul National University, Seoul, 151-742, Republic of Korea*
(Received 21 September 2007; revised manuscript received 4 August 2008; published 3 October 2008)

The stability of a dislocation defect with two pentagon-heptagon (5-7) pairs in a graphene layer is investigated within first-principles density-functional theory scheme. It is found that the structure of the dislocation defect with two 5-7 pairs becomes more stable than a local haeckelite structure which is composed of defect units of three pentagons and three heptagons (555-777 defect) when the number of vacancy units is ten and over. The simulation study of scanning tunneling microscopy reveals that the 5-7 pair defects perturb the wave functions of electrons near Fermi level to produce the $(\sqrt{3}\times\sqrt{3})R30^0$: a superlattice pattern.

DOI: 10.1103/PhysRevB.78.165403 PACS number(s): 61.50.Ah, 61.72.J−, 81.05.Uw, 71.15.Mb

I. INTRODUCTION

Graphene has been one of the most remarkable materials in the past few years in terms of academic interests[1,2] and applicability to the semiconductor industry.[3] Defects have been known to change the physical and chemical properties of graphite significantly,[4–6] and recent improvements in microscope technologies make it possible to visualize the artificial defects induced by electron or ion-beam irradiation on graphene and carbon nanotubes at the atomic scale level.[7–10] Recently, a dislocation defect in which one carbon zigzag chain is missing from a pristine graphene was found under *in situ* high-resolution transmission electron microscopy by Hashimoto *et al.*[7] In their study, the dislocation has been reported to contain a pentagon-heptagon (5-7) pair defect. The 5-7 pair defect plays an important role in the formation of carbon nanotube junctions.[11,12] The 5-7 pair defects are suggested to be responsible for a kink structure which is generated in carbon nanotubes under tensile strain.[13,14] It has also been reported through tight-binding molecular-dynamics simulation (TBMDS) that the reconstruction of vacancy defects in a single wall carbon nanotube results in the formation of two 5-7 pair defects and the partial reduction of the diameter of the nanotube.[15,16]

On the other hand, double vacancy defects in graphene have been reported to undergo a structural change from a defect structure made up of two pentagons and one octagon (5-8-5) to a defect structure of three pentagons and three heptagons (555-777) which is slightly lower in energy.[17] The 555-777 defect was also proposed to be a basic unit of the haeckelite structure[18] (see Fig. 2 for the details of the structure). Recent TBMDS has demonstrated that four vacancy units are reconstructed into two neighboring 555-777 defects and some collective 555-777 defects form a local haeckelite structure in a graphene.[19] The 555-777 defect was also suggested to be a stable structure of double vacancy in single-walled carbon nanotubes of a large diameter.[20] However, if many vacancy defects are reconstructed into the collective 555-777 defects and form a local haeckelite structure in a graphene, a large strain should be induced by the increase in nonhexagonal rings and the structure could be reconstructed into the other structure of lower total energy. In this paper, we suggest the dislocation with two 5-7 pair defects [see Figs. 1(g) and 1(h) for the details of structures] as the defect structure of lower total energy in a graphene and test the stability comparing it to the local haeckelite structure composed of 555-777 defects.

II. CALCULATIONAL METHOD

Total-energy calculations are performed within first-principles density-functional theory scheme.[21] We use the SIESTA code within the local-density approximation employing the Ceperley-Alder exchange-correlation functional[22] and the norm-conserving Troullier-Martins pseudopotential.[23] The double zeta atomic basis set is used with the mesh cutoff of 200 Ry for the real grid mesh. Some important results are crosschecked with the Vienna *ab initio* simulation package (VASP) code in which the plane-wave basis set[24] is employed. In this calculation, the PW91 generalized gradient approximation[25] is used and the basis set consists of plane waves with the kinetic energy up to 21.1 Ry. We choose one k point (Γ) in the two-dimensional irreducible Brillouin zone. An orthorhombic supercell, which contains a 12 Å vacuum region of z axis and vacancy defects on a graphene of 448 carbon atoms spanning two-dimensional x and y space, is chosen as a unitcell. In order to obtain on optimized structure, all atoms are fully relaxed until the force is smaller than 0.04 eV/Å.

III. RESULT AND DISCUSSION

First, we make four graphene layers containing zigzag chains of four, six, eight, and ten vacancy units, respectively, as shown in Figs. 1(a)–1(d). Those are relaxed by the steepest-descent method within the first-principles density-functional theory scheme. Figures 1(e)–1(h) show the relaxed geometries. In this relaxation, it is observed that for the case of four and six vacancy units, two pentagons are formed by bonding among carbon atoms (atoms 1–2 and 3–4 in Figs. 1(a) and 1(b)] at both ends of defect chains as shown in Figs. 1(e) and 1(f). For the case of eight vacancy units, after the formation of pentagons, the formation of a bond between two carbon atoms [atom 7–8 in Fig. 1(c)] with dangling

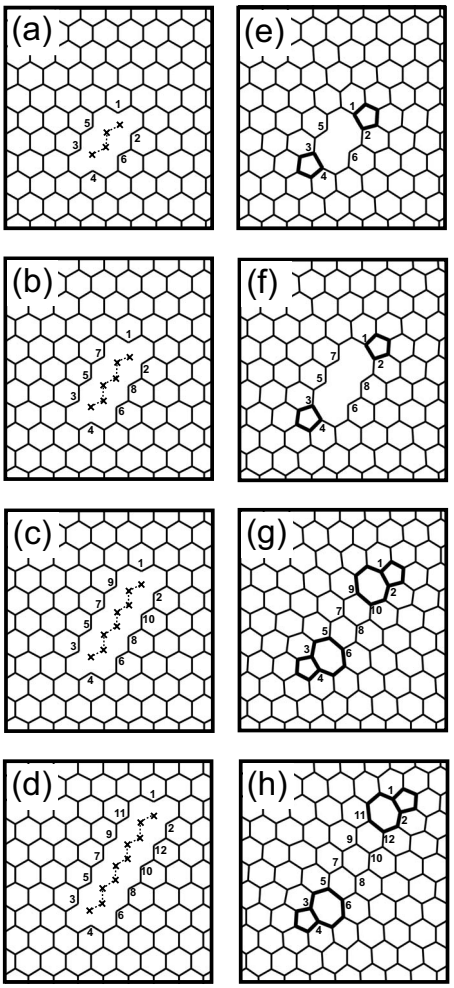

FIG. 1. The initial geometries [(a)–(d)] and the relaxed geometries [(e)–(h)] of graphenes containing four [(a) and (e)], six [(b) and (f), eight [(c) and (g)], and ten [(d) and (h)] vacancy units. Crosses and dashed lines in (a)–(d) indicate the positions of carbon vacancies and zigzag chains of carbon vacancies, respectively. The bold lines in (e)–(h) indicate pentagon and heptagon rings formed by the structural relaxation. See the text for numbers.

bonds is observed and it is followed by the formation of bonds between atoms 5–6 and 9–10 resulting in the formation of two 5-7 pair defects at both ends of the dislocation as shown in Fig. 1(g). For the case of ten vacancy units, the initial geometry [Fig. 1(d)] is relaxed to the dislocation with two 5-7 pair defects due to the full saturation of dangling bonds as shown in the final geometry of Fig. 1(h).

The stability of the dislocation defect with two 5-7 pairs is compared with that of the local haeckelite structure composed of 555-777 defect units by the total-energy calculation. Figure 2 shows the relaxed geometries of various local haeckelite structures[26] depending on the number of vacancy units. Since one 555-777 defect unit is formed by the generation of two vacancy units on a graphene, the local haeckelite structures showed in Figs. 2(a)–2(d) contain four, six, eight, and ten vacancy units, respectively. We test the stability of the dislocation defect with two 5-7 pairs comparing it with the local haeckelite structure by the calculation of formation energies. In this study, the formation energy E_{form} is defined[27] as

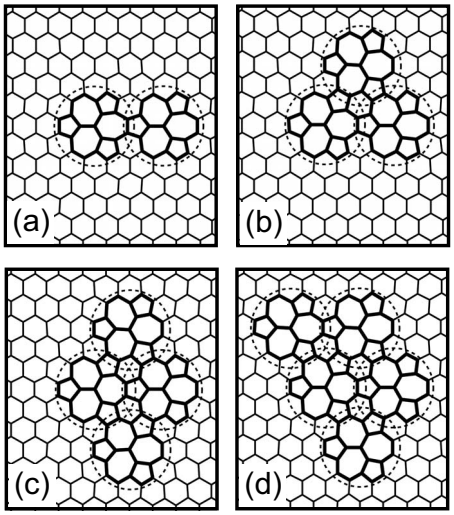

FIG. 2. The relaxed geometries of local haeckelite structures by (a) four, (b) six, (c) eight, and (d) ten vacancy units. Bold lines indicate pentagon and heptagon rings. Dashed circles indicate the 555-777 defect units.

$$E_{\text{form}}[N-n] = E_{\text{tot}}[N-n] - (N-n)\mu_{\text{gra}}, \tag{1}$$

where N is the total number of carbon atoms in a pristine graphene which fit to our unitcell, n is the number of vacancies, $E_{\text{tot}}[N-n]$ is the total energy of reconstructed graphene with the $N-n$ carbon atoms, and μ_{gra} is the chemical potential for a carbon atom calculated as the energy per atom for a pristine graphene. Figure 3 shows formation energies of the dislocation defect with two 5-7 pairs and the local haeckelite structure depending on the number of vacancy units. Interestingly, the formation energy of local haeckelite structures increases linearly as the number of vacancy units increases, which indicates that the additional formation of 555-777 defect gives rise to the linear increase in formation energy, and the increase in the formation energy per an additional 555-777 defect is about 6.0 eV. On the contrary, the formation energy of dislocation defect with two 5-7 pairs shows a dif-

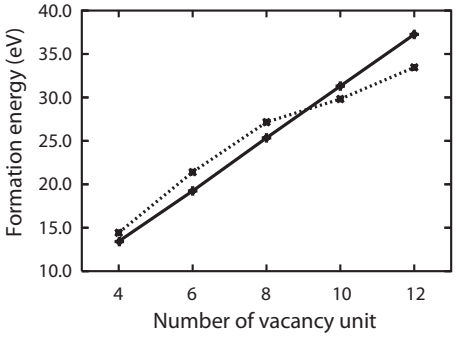

FIG. 3. Formation energy per one carbon atom in case of the local haeckelite structure (solid line) and the dislocation defect (dotted line) with two 5-7 pairs as a function of the number of vacancy units. Crosses indicate data points.

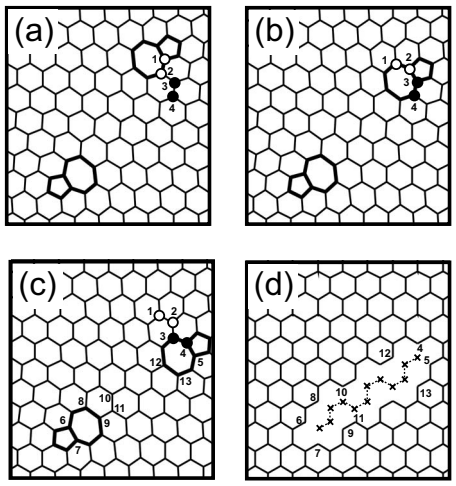

FIG. 4. Diffusion of a 5-7 pair defect by the 90° rotation of carbon dimers. (a) The structure shows two 5-7 pair defects formed by the zigzag chain of twelve vacancy units. (b) One 5-7 pair defect is diffused by the 90° rotation of carbon dimer indicated by open circles. (c) The 5-7 pair defect is diffused again by the 90° rotation of carbon dimer indicated by filled circles. (d) The structure shows the missing armchair chain of 12 carbon atoms. This structure could be reconstructed into the structure showed in (c) by the formation of bonds among the carbon atoms with dangling bonds.

ferent pattern from that of the local haeckelite structure. As the number of vacancy units increases from six to eight, the structure is stabilized by the formation of bonds among carbon atoms with dangling bonds as shown in Figs. 1(f) and 1(g) and the increase rate in the formation energy has lowered as shown in Fig. 3. As the number of vacancy units increases to ten, the dislocation structure with two 5-7 pair defects is more stabilized by the full saturation of dangling bonds as shown in Fig. 1(h). The full saturation of dangling bonds is verified by the comparison of bond lengths. The bond length (1.73 Å) between atoms 5 and 6 in Fig. 1(g) is larger than that (1.68 Å) between atoms 5 and 6 in Fig. 1(h), which indicates that the saturation of dangling bonds in the dislocation structure with eight vacancy units is not complete as compared with that of ten vacancy units. We also relax the dislocation structure of twelve vacancy units [Fig. 4(a)] to test the completeness of dangling bonds saturation. In the relaxation, the bond length between atoms 8 and 9 in Fig. 4(a) is found to be 1.67 Å, which is very similar to that in the dislocation structure with ten vacancy units. Thus, when the number of vacancy units is ten, the dangling bonds are almost fully saturated and the increase rate in the formation energy is more lowered as shown in Fig. 3. The formation energy of the dislocation defect becomes lower than that of the local haeckelite structure as the number of vacancy units increases over ten. The formation energy of the dislocation with 5-7 pair defects increases by 3.9 eV when the number of vacancy units increases from ten to twelve. From eight vacancy units to ten vacancy units, the formation energy is dramatically changed by the full saturation of dangling bonds as shown in Fig. 3. However, when the number of vacancy units is over ten, no more dramatic change in the formation energy would be observed due to the complete saturation of dangling bonds. As the number of vacancy units increases over ten, one hexagon between two 5-7 pair defects increases whenever two vacancy units are formed [We can confirm the increase of one hexagon between two 5-7 pair defects by comparing Fig. 1(h) with Fig. 4(a).] and the hexagons between two 5-7 pair defects are strained by the saturation of dangling bonds differently to the normal hexagons in the pristine graphene. As the number of strained hexagons increases, the formation energy would increase linearly. In the calculation with a larger unit cell containing a graphene which consists of 720 carbon atoms, the increase in the formation energy in the dislocation structure from ten to twelve vacancy units is found to be 2.9 eV which is smaller than that (3.9 eV) in the original unit cell which contains 448 carbon atoms. The formation energy is considered to be reduced by further relaxation in the larger unit cell, which indicates that the formation energy is sensitive to the size of unit cell, and the dislocation defect has a long-range interaction on a graphene. As the number of vacancy units increases, a larger unit cell should be demanded to reduce the strain and to relax the dislocation defect fully. However, for the local haeckelite structure, the increase in the formation energy is found to be 5.8 eV when the number of vacancy units increases from ten to twelve in the large unit cell with 720 carbon atoms and it is not sensitive to the size of unit cell. Even though it is difficult to find the saturated value of the formation energy due to the high cost from the calculation with a large unit cell, it is confirmed that the increase in the formation energy per additive two vacancy units in case of the dislocation defect is much smaller than that in case of the local haeckelite structure.

We also consider the other type of dislocation by diffusion of a 5-7 pair defect. The diffusion of a 5-7 pair is induced by 90° rotations of carbon dimers as shown in Fig. 4. Figure 4(a) shows the dislocation with two 5-7 pair defects, which is formed by the reconstruction of a zigzag vacancy chain with twelve vacancy units. The 90° rotation of a dimer (atoms 1–2) in Fig. 4(a) also gives rise to the other type of dislocation as shown in Fig. 4(b). The sequential 90° rotation of a dimer (atoms 3–4) also creates the other type of dislocation [Fig. 4(c)], which could be formed by the reconstruction of an armchair vacancy chain as shown in Fig. 4(d). The structure in Fig. 4(d) could be reconstructed into the structure in Fig. 4(c) by the bond formation of atoms 4–5, 6–7, 8–9, 10–11, …, and 12–13. In our calculation, the dislocation structure in Fig. 4(a) is the most stable and the total energy is lower than that of the dislocation structures in Figs. 4(b) and 4(c) by 0.1 and 0.4 eV, respectively.

Another interesting issue is the $(\sqrt{3}\times\sqrt{3})R30^0$ superlattice patterns, which are observed in scanning tunneling microscopy (STM) images of various defects on the graphite surface.[5,8,28,29] It has been suggested that such a kind of a long-range electronic perturbation is derived from a point defect by a certain adsorbate, such as the Friedel oscillation on a metal surface, and the $(\sqrt{3}\times\sqrt{3})R30^0$ pattern in the threefold symmetric STM image is due to the adsorbate observed in some experiments.[8,28] However, the $(\sqrt{3}\times\sqrt{3})R30^0$ superlattice patterns without the threefold symmetry were also observed in STM images of some defect structures after the inert gas ion irradiation.[29–31] These ex-

perimental results corroborate that even if there is no adsorbate, the $(\sqrt{3}\times\sqrt{3})R30^0$ superlattice patterns could arise when the certain local geometrical defects are formed at a graphite surface after the diffusion process of vacancies during the irradiation. We perform the simulation of the STM topographic image for the structure of the dislocation defect with two 5-7 pairs. According to the Tersoff-Hamann method,[32] the topographic image is obtained by calculating local density of states (LDOS) with a sample bias voltage of −0.5 V. Figure 5 shows the result and the corresponding atomic structure of dislocation defect with two 5-7 pairs. The 5-7 pair defects strongly enhance the LDOS above them and the simulated STM image has no threefold symmetry. It is well known that the tunneling current maxima in the typical STM images of the graphite surface occur on the sublattice sites which have no neighbors in the lower layer due to interlayer interaction.[33,34] However, it is interesting that such typical patterns are observable in the STM image of a single graphene layer and the $(\sqrt{3}\times\sqrt{3})R30^0$ patterns near 5-7 pair defects are also found. This result demonstrates that the 5-7 pair defects act as scattering centers for wave functions of electrons near the Fermi level to produce the $(\sqrt{3}\times\sqrt{3})R30^0$ patterns. Our simulated STM image suggests that the $(\sqrt{3}\times\sqrt{3})R30^0$ patterns without the threefold symmetry in experiments[29–31] could originate from the 5-7 pair defects. Another interesting difference from STM images[35,36] of some defect structures in graphene is the missing of every other atom which is also found in the STM image of multiplayer graphite. It is considered to be due to the 5-7 pair defects and need to be studied in the electronic structure further.

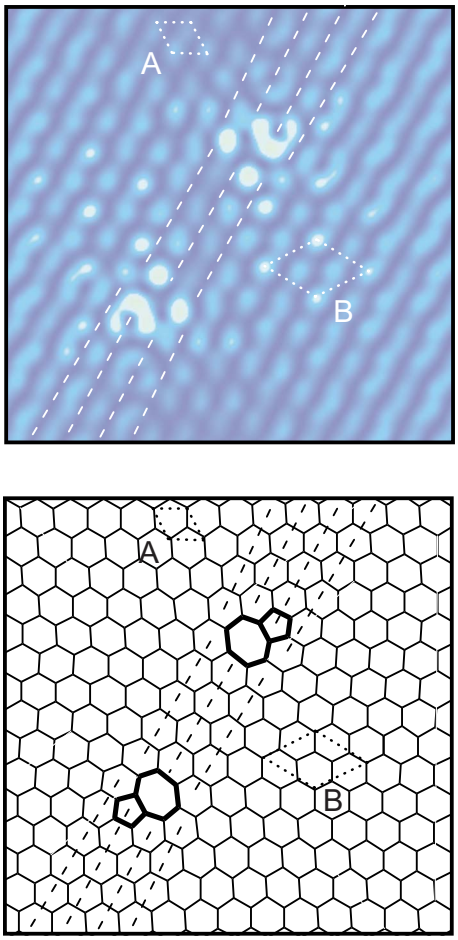

FIG. 5. (Color online) The simulated STM image (upper) and its atomic structure (lower). (a) The small dotted rhombus indicates the typical 1×1 hexagonal pattern of a graphene surface and (b) the large dotted rhombus indicates the $(\sqrt{3}\times\sqrt{3})R30^0$ pattern. Dashed lines show a deficiency of one carbon chain between two 5-7 pair defects.

IV. SUMMARY

It is found by the total-energy calculation that the dislocation defect with two 5-7 pairs is preferred to the local haeckelite structure composed of collective 555-777 defects when the number of vacancy units increases to more than ten. It is also found that the type of the 5-7 pair defect with a missing zigzag carbon chain is energetically more stable than other types of 5-7 pair defect including the type of the missing armchair carbon chain. The simulated STM image also shows the $(\sqrt{3}\times\sqrt{3})R30^0$ superlattice pattern around the 5-7 pair defects.

ACKNOWLEDGMENTS

We acknowledge the support of the KOSEF grant funded by MEST (Center for Nanotubes and Nanostructured Composites), the Korea Research Foundation with Grants No. KRF-2005-070-C00041 and No. KRF-2005-041-D00406, and the Korean Government MOEHRD Basic Research Fund with Grant No. KRF-2006-341-C000015. G.D.L. would like to acknowledge the support from KISTI under the Strategic Supercomputing Applications Support Program. The use of the computing system of the Supercomputing Center is also appreciated.

[1] K. S. Novoselov, A. K. Geim, S. V. Morozov, D. Jiang, M. I. Katsnelson, I. V. Grigorieva, S. V. Dubonos, and A. A. Firsov, Nature (London) **438**, 197 (2005).
[2] Y. Zhang, Y.-W. Tan, H. L. Stormer, and P. Kim, Nature (London) **438**, 201 (2005).
[3] A. K. Geim and K. S. Novoselov, Nat. Mater. **6**, 183 (2007).
[4] P. O. Lehtinen, A. S. Foster, A. Ayuela, A. Krasheninnikov, K. Nordlund, and R. M. Nieminen, Phys. Rev. Lett. **91**, 017202 (2003).
[5] H. A. Mizes and J. S. Foster, Science **244**, 559 (1989).
[6] K. F. Kelly, D. Sarkar, G. D. Hale, S. J. Oldenburg, and N. J. Halas, Science **273**, 1371 (1996).
[7] A. Hashimoto, K. Suenaga, A. Gloter, K. Urita, and S. Iijima, Nature (London) **430**, 870 (2004).

[8] K. F. Kelly and N. J. Halas, Surf. Sci. **416**, L1085 (1998).
[9] H. Kim, J. Lee, S.-J. Kahng, Y.-W. Son, S. B. Lee, C.-K. Lee, J. Ihm, and Y. Kuk, Phys. Rev. Lett. **90**, 216107 (2003).
[10] K. Suenaga, H. Wakabayashi, M. Koshino, Y. Sato, K. Urita, and S. Iijima, Nat. Nanotechnol. **2**, 358 (2007).
[11] L. Chico, Vincent H. Crespi, Lorin X. Benedict, Steven G. Louie, and Marvin L. Cohen, Phys. Rev. Lett. **76**, 971 (1996).
[12] J.-C. Charlier, T. W. Ebbesen, and Ph. Lambin, Phys. Rev. B **53**, 11108 (1996).
[13] J. Y. Huang, S. Chen, Z. F. Ren, Z. Q. Wang, D. Z. Wang, M. Vaziri, Z. Suo, G. Chen, and M. S. Dresselhaus, Phys. Rev. Lett. **97**, 075501 (2006).
[14] F. Ding, K. Jiao, M. Wu, and B. I. Yakobson, Phys. Rev. Lett. **98**, 075503 (2007).
[15] G.-D. Lee, C. Z. Wang, J. Yu, E. Yoon, N.-M. Hwang, and K. M. Ho, Phys. Rev. B **76**, 165413 (2007).
[16] G.-D. Lee, C. Z. Wang, E. Yoon, N.-M. Hwang, and K. M. Ho, Appl. Phys. Lett. **92**, 043104 (2008).
[17] G.-D. Lee, C. Z. Wang, E. Yoon, N.-M. Hwang, D.-Y. Kim, and K. M. Ho, Phys. Rev. Lett. **95**, 205501 (2005).
[18] H. Terrones, M. Terrones, E. Hernández, N. Grobert, J.-C. Charlier, and P. M. Ajayan, Phys. Rev. Lett. **84**, 1716 (2000).
[19] G.-D. Lee, C. Z. Wang, E. Yoon, N.-M. Hwang, and K. M. Ho, Phys. Rev. B **74**, 245411 (2006).
[20] R. G. Amorim, A. Fazzio, A. Antonelli, F. D. Novaes, and A. J. R. Silva, Nano Lett. **7**, 2459 (2007).
[21] W. Kohn and L. J. Sham, Phys. Rev. **140**, A1133 (1965).
[22] D. M. Ceperley and B. J. Alder, Phys. Rev. Lett. **45**, 566 (1980).
[23] N. Troullier and J. L. Martins, Phys. Rev. B **43**, 1993 (1991).
[24] G. Kresse and J. Furthmüller, Phys. Rev. B **54**, 11169 (1996).
[25] J. P. Perdew and Y. Wang, Phys. Rev. B **33**, 8800 (1986).
[26] There can be some alternative configurations of local haeckelites depending on the arrangement of 555-777 defects. In our calculations, the maximum of those formation energy differences is found to be less than 0.3 eV.
[27] Charge is not considered in the formation energy. In carbon system, the charge effect is unlikely to change the relative energy and structure of defect structure, J. M. Carlsson and M. Scheffler, Phys. Rev. Lett. **96**, 046806 (2006).
[28] P. Ruffieux, M. Melle-Franco, O. Gröning, M. Bielmann, F. Zerbetto, and P. Gröning, Phys. Rev. B **71**, 153403 (2005).
[29] B. An, S. Fukuyama, K. Yokogawa, and M. Yoshimura, Jpn. J. Appl. Phys., Part 1 **39**, 4347 (2000).
[30] J. R. Hahn and H. Kang, Phys. Rev. B **60**, 6007 (1999).
[31] Z. Osváth, G. Vértesy, L. Tapasztó, F. Wéber, Z. E. Horváth, J. Gyulai, and L. P. Biró, Phys. Rev. B **72**, 045429 (2005).
[32] J. Tersoff and D. R. Hamann, Phys. Rev. B **31**, 805 (1985).
[33] D. Tománek, S. G. Louie, H. J. Mamin, D. W. Abraham, R. E. Thomson, E. Ganz, and J. Clarke, Phys. Rev. B **35**, 7790 (1987).
[34] O. V. Sinitsyna and I. V. Yaminsky, Russ. Chem. Rev. **75**, 23 (2006).
[35] G. M. Rutter, J. N. Crain, N. P. Guisinger, T. Li, P. N. First, and J. A. Stroscio, Science **317**, 219 (2007).
[36] H. Amara, S. Latil, V. Meunier, Ph. Lambin, and J. C. Charlier, Phys. Rev. B **76**, 115423 (2007).